Structural Engineering and Mechanics, Vol. 31, No. 6 (2009) 639-662
DOI: http://dx.doi.org/10.12989/sem.2009.31.6.639

Earthquake response of isolated cable-stayed bridges under spatially varying ground motions

Sevket Ates†

Department of Civil Engineering, Karadeniz Technical University, Trabzon, 61080, Turkey

Kurtulus Soyluk‡

Department of Civil Engineering, Gazi University, Maltepe, Ankara, 06570, Turkey

A. Aydin Dumanoglu‡†

Department of Civil Engineering, Karadeniz Technical University, Trabzon, 61080, Turkey

Alemdar Bayraktar‡‡

Department of Civil Engineering, Karadeniz Technical University, Trabzon, 61080, Turkey

(Received July 16, 2007, Accepted March 12, 2009)

Abstract. A comprehensive investigation of the stochastic response of an isolated cable-stayed bridge subjected to spatially varying earthquake ground motion is performed. In this study, the Jindo Bridge built in South Korea is chosen as a numerical example. The bridge deck is assumed to be continuous from one end to the other end. The vertical movement of the stiffening girder is restrained and freedom of rotational movement on the transverse axis is provided for all piers and abutments. The longitudinal restraint is provided at the mainland pier. The A-frame towers are fixed at the base. To implement the base isolation procedure, the double concave friction pendulum bearings are placed at each of the four support points of the deck. Thus, the deck of the cable-stayed bridge is isolated from the towers using the double concave friction pendulum bearings which are sliding devices that utilize two spherical concave surfaces. The spatially varying earthquake ground motion is characterized by the incoherence and wave-passage effects. Mean of maximum response values obtained from the spatially varying earthquake ground motion case are compared for the isolated and non-isolated bridge models. It is pointed out that the base isolation of the considered cable-stayed bridge model subjected to the spatially varying earthquake ground motion significantly underestimates the deck and the tower responses.

Keywords: spatially varying ground motion; wave-passage effect; incoherence effect; base isolation; isolated bridge; cable-stayed bridge; double concave friction pendulum.

† Assistant Professor, Corresponding author, E-mail: sates@ktu.edu.tr
‡ Associate Professor, E-mail: ksoyluk@gazi.edu.tr
‡† Professor, E-mail: aduman@ktu.edu.tr
‡‡ Professor, E-mail: alemdar@ktu.edu.tr

1. Introduction

Base isolation of structures is a viable solution for earthquake protection. Using base isolation, responses of structures such as buildings, bridges, tanks and pipelines are shifted to a higher fundamental period. Base isolations have been commonly used recently in the construction of new structures and retrofitting of existing structures. The double concave friction pendulum (DCFP) bearing is an innovative and viable isolation system that is becoming widespread application for the earthquake protection of structures. The DCFP consists of two spherical stainless steel surfaces and an articulated slider covered by a Teflon-based high bearing capacity composite material. The concave surfaces may have the same radii of curvature. Also, the coefficient of friction on the two concave surfaces may be the same or not.

Experimental and analytical results on the behaviour of a system having concave surfaces of both equal and unequal radii and both equal and unequal coefficient of friction at the upper and lower sliding surfaces were presented by Tsai *et al.* (2006). Constantinou (2004), Fenz and Constantinou (2006) described the principles of operation of the DCFP bearing and presented the development of the force-displacement relationship based on equilibrium. The theoretical force–displacement relationship was verified through characterization testing of bearings with sliding surfaces having the same and then different radii of curvature and coefficients of friction. Finally, practical considerations for analysis and design of DCFP bearings were presented. Hyakuda *et al.* (2001) presented the description and response of a seismically isolated building in Japan where DCFP bearings are utilized. Zayas *et al.* (1989) introduced one of the most effective sliding isolation systems, namely the friction pendulum system, which utilizes friction to dissipate the transmitted energy to the structure.

The dynamic responses of extended structures like bridges, pipelines and dams are significantly affected by spatially varying earthquake ground motions. The earthquake response analysis of long-span non-isolated bridges subjected to spatially varying earthquake ground motions was investigated by Perotti (1990), Harichandran *et al.* (1988), Zembaty and Rutenberg (1998) and Zerva (1991). Recently, Soyluk and Dumanoglu (2004) carried out stochastic analysis of non-isolated cable-stayed bridges for delayed support excitations and concluded that any seismic analysis of even moderately long span non-isolated cable-stayed bridges requires the consideration of the wave-passage effects. Additionally, Soyluk *et al.* (2004) presented various random vibration and deterministic analyses of non-isolated cable-stayed bridges to asynchronous ground motion. It was found that the structural response values show important amplifications depending on the decreasing ground motion wave velocities. Ates *et al.* (2005, 2006) studied the stochastic response of isolated highway bridges by friction pendulum systems to spatially varying earthquake ground motions and reported that friction pendulum systems have important effects on the stochastic responses of bridges to spatially varying earthquake ground motions. Lou and Zerva (2005) investigated the effects of the spatially varying earthquake ground motions on the seismic response of a skewed, multi-span and RC highway bridge.

Due to the flexibility of cable-stayed bridges, the deck has a large displacement response under earthquake ground motions. Therefore, the connections between the deck and the tower of cable-stayed bridges become important for earthquake ground motions. The connection between the tower and the deck will reduce the deck displacement but will increase the base shear of the tower. In order to overcome this issue, base isolation technique is considered by providing isolation bearings at the supports of the deck. So far, very limited research was conducted for the effectiveness of

seismic isolation systems on cable-stayed bridge systems (Ali and Abdel-Ghaffar 1994, Wesolowsky and Wilson 2003, Soneji and Jangid 2006). These studies were performed for uniform ground motions and showed that the isolation in cable-stayed bridges could significantly reduce the seismically induced forces at the towers of the bridges. However, the isolation system increased the horizontal displacement responses of the deck. Jung *et al.* (2004) proposed a hybrid control strategy combining passive and semi-active control systems for the seismic protection of cable-stayed bridges. It was reported that the performance of the proposed hybrid control strategy was quite effective in protecting seismically excited cable-stayed bridges. Soneji and Jangid (2006, 2007) examined the efficacy of hybrid control system for the seismic protection of cable-stayed bridges subjected to near-field ground motion and reported that the hybrid system significantly enhances the seismic performance of cable stayed bridges.

Although cable-stayed bridges have been analysed for different isolation systems, the effects of the isolation mechanisms on the stochastic response of cable-stayed bridges when subjected to spatially varying ground motions are not taken into account so far. The objective of this paper is to determine the relative importance of using double concave friction pendulum bearings for the isolation of a cable-stayed bridge system in the stochastic earthquake response analysis when the bridge system is subjected to the spatially varying earthquake ground motion. For this purpose, total responses at the deck and the towers are compared for the isolated and non-isolated bridge models. Frequencies of occurrences of the deck bending moments are also presented.

2. Cable-stayed bridge model

In this study, the Jindo Bridge, shown in Fig. 1, built in South Korea is chosen as a numerical example. Jindo Bridge has three spans; the main span of 344 m and two side spans of 70 m. The stays are arranged in a fan configuration and converged at the top of the A-shaped frame towers. The stiffening girder and the towers of the Jindo Bridge were made from steel. A 2% damping coefficient is adopted for the response calculations. Because the purpose of this study is to compare the results of the spatially varying ground motion rather than to study the effect of bridge geometry, only one mathematical model is considered.

The stiffening girder is of hexagonal shape and continuous from one end to the other. In cable-stayed bridge systems, continuous stiffening girders are preferred at most. For the proper

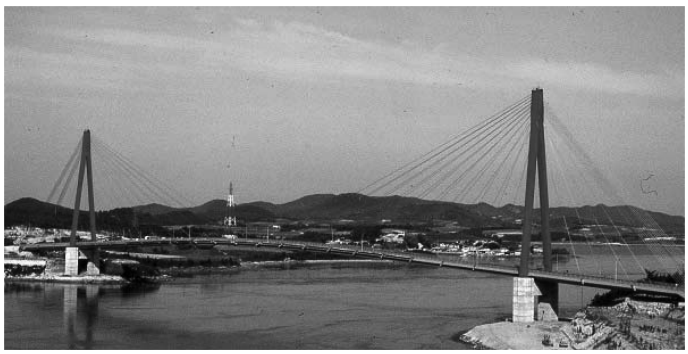

Fig. 1 The Jindo Bridge

functioning of the bridge deck it is necessary to provide transverse restraint at each pier and abutment and longitudinal restraint at one pier or abutment. The vertical movement of the girder is restrained and freedom of rotational movement on the transverse axis is provided for all pier and abutments. The longitudinal restraint is provided at the mainland pier.

In order to investigate the stochastic response of the Jindo Bridge, two-dimensional mathematical model is used for calculations. It has been shown that a two-dimensional analysis of the cable-stayed bridge provides natural frequencies and mode shapes which are in close agreement with those obtained by the three-dimensional analysis (Garevski *et al.* 1988). Therefore a two-dimensional analysis is carried out in the vertical direction plane of the Jindo Bridge in order to achieve the stochastic response to spatially varying earthquake forces. The fact that this 2-D model has a relatively small number of degrees of freedom makes it more attractive by saving on computer time. Obviously, if actual design values for the responses are desired 3-D model should be taken into account. The bridge is modelled using beam-column elements for deck and towers and truss elements for cables. The chosen finite element model is represented by 420 degrees of freedom. The stiffening girder and towers are represented by 139 beam elements.

As known, the dynamic behaviour of cable-stayed bridges depends on the connection type used between the tower and deck. If the deck is swinging freely at the towers, the resulting dynamic forces will be very small. This connecting type will result very flexible bridge system under existing loads. However, rigid connection between the deck and tower will control the movements of the deck but will result large dynamic forces under earthquake ground motions. Therefore, in this study the connection of the deck to the tower of the non-isolated bridge system is provided by elastic links to control the bridge responses. For the isolated bridge system, isolation bearing are provided at the support points of the deck.

Although non-linear analysis of cable-stayed bridges reflects a more realistic behaviour of the bridge, linear dynamic analysis was found to be economical and justified for moderately long span bridges without losing the accuracy to a great extent (Morris 1974, Fleming and Egeseli 1980, Nazmy and Abdel-Ghaffar 1987, 1990, 1992). Since the cable-stayed bridge model under study has a centre span of 344 m, a linear dynamic analysis should be sufficient. The cable stays are modelled with 28 truss elements and the non-linearity of the inclined cable stays is considered with an equivalent modulus of elasticity.

Since the primary objective of this study is to perform a parametrical study associated with the spatial variability of ground motions and its effects on the response of base isolated cable-stayed bridges, the soil-structure interaction is not considered. Although the soil-structure interaction is important for long span bridges (Betti *et al.* 1993), the non-consideration of the soil-structure interaction in this study is caused by the avoidance to model absorbing boundaries in the dynamic analysis.

3. Double concave friction pendulum bearings

The double concave friction pendulum (DCFP) bearings are made of two concave surfaces which are called as upper and lower and shown in Fig. 2 (Constantinou 2004, Fenz and Constantinou 2006). The concave surfaces may have the same radii of curvature. Also, the coefficient of friction on the two concave surfaces may be the same or not. The maximum displacement capacity of the bearing is $2d$, where d is the maximum displacement capacity of a single concave surface. Note that

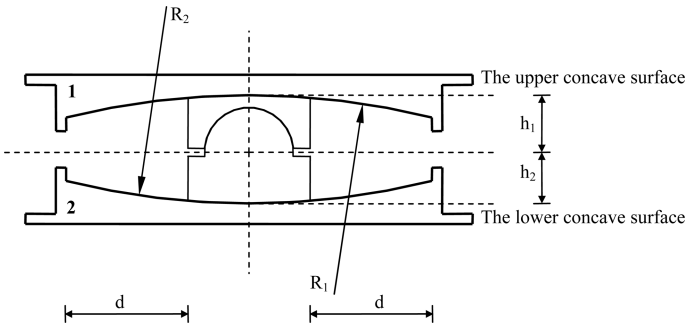

Fig. 2 The double concave friction pendulum bearing having equal radii of curvature

due to rigid body and relative rotation of the slider, the displacement capacity is actually slightly different from $2d$. The force-displacement relationship for the DCFP bearing is given by the following equation

$$F = \left(\frac{W}{R_1 - h_1 + R_2 - h_2}\right) v_b + \left(\frac{F_{f1}(R_1 - h_1) + F_{f2}(R_2 - h_2)}{R_1 - h_1 + R_2 - h_2}\right) \tag{1}$$

where W is the vertical load, R_1 and R_2 are radii of the two concave surfaces, h_1 and h_2 are the part heights of the articulated slider, v_b is the total displacement (bearing displacement) and the sum of the displacements on the upper and lower surfaces are given by

$$v_b = 2d = v_{b1} + v_{b2} \tag{2}$$

herein v_{b1} and v_{b2} are the displacements of the slider on the upper and lower concave surfaces, respectively, and the individual displacements on each sliding surfaces are

$$v_{b1} = \left(\frac{F - F_{f1}}{W}\right)(R_1 - h_1) \tag{3}$$

$$v_{b2} = \left(\frac{F - F_{f2}}{W}\right)(R_2 - h_2) \tag{4}$$

in Eqs. (3) and (4), F_{f1} and F_{f2} are the friction forces on the concave surfaces 1 and 2, respectively. The forces are given by

$$F_{f1} = \mu_1 W \text{sgn}(\dot{v}_{b1}) \tag{5}$$

$$F_{f2} = \mu_2 W \text{sgn}(\dot{v}_{b2}) \tag{6}$$

where μ_1 and μ_2 are the coefficient of friction on the concave surfaces 1 and 2, respectively; $\dot{v}_{b1}$ and $\dot{v}_{b2}$ are sliding velocities at the upper and lower surfaces, respectively; sgn (.) denotes the signum function. Most applications of the DCFP bearings will likely utilize concave surfaces of equal radii, namely, $R_1 = R_2$. Parts heights of the articulated slider h_1 and h_2 are nearly equal in most cases. Thus, the effective coefficient of friction is equal to the average of μ_1 and μ_2, and is given by

$$\mu_e = \frac{\mu_1(R_1 - h_1) + \mu_2(R_2 - h_2)}{R_1 + R_2 - h_1 - h_2} \tag{7}$$

In this study, $R_1 - h_1 = R_2 - h_2 = 1.60$ m and μ_e is calculated as 0.05 by Eq. (7) due to variability in properties $\mu_1 = 0.045$ and $\mu_2 = 0.055$.

In Eq. (1), the first term is the stiffness of the pendulum component (spring forces) and the second term is the stiffness of the friction component. The natural period of vibration is given by the following equation

$$T = 2\pi\sqrt{\frac{R_1 + R_2 - h_1 - h_2}{g}} = 2\pi\sqrt{\frac{R_e}{g}} \tag{8}$$

where g is the acceleration of gravity; R_e is the effective radius of curvatures. Eq. (8) shows that the natural period of vibration is independent of mass, but it is controlled by the selection of the radius of the spherical concave surfaces. In this study, the period of the isolation system is calculated as 2.75 sec depending on the radii of the two concave surfaces. The important parameter is employed as $R_e = R_1 + R_2 - h_1 - h_2 = 1.88$ m. The lateral restoring stiffness of the DCFP bearing (spring forces) is given by the following equation

$$k_b = \frac{W}{R_1 + R_2 - h_1 - h_2} \tag{9}$$

It is also shown in Eq. (9) that the stiffness of the pendulum depends on the weight carried by bearing. The coefficient of the friction of the two concave surfaces depend on the bearing pressure and given by Eq. (10)

$$\mu_{1,2} = f_{\max} - (f_{\max} - f_{\min})e^{(a|\dot{v}_b|)} \tag{10}$$

where $f_{\max}$ and $f_{\min}$ are the maximum and minimum mobilized coefficients of friction, respectively; and a is a parameter that controls the variation of the coefficient with the velocity of sliding. In this study $f_{\max}$, $f_{\min}$ and a are used as 0.0572, 0.0087 and 50 s/m, respectively at 70 MPa bearing pressure (Constantinou 2004).

4. Governing equation of motion

The equation of motion of a non-isolated structural system can be written as

$$[M]\{\ddot{v}\} + [C]\{\dot{v}\} + [K]\{v\} = \{F\} \tag{11}$$

where $[M]$, $[C]$ and $[K]$ are the mass, damping and stiffness matrices, respectively; $\{\ddot{v}\}, \{\dot{v}\}$ and $\{v\}$ are vectors of total accelerations, velocities and displacements, respectively and $\{F\}$ is a vector of input forces.

The degrees of freedom can be defined as known and unknown. The known degrees of freedom are associated with those of the structure-foundation interface. The unknowns are related to degrees of freedom of the structure. The former degrees of freedom will be denoted henceforth as the vector $\mathbf{v}_g$, and the latter as $\mathbf{v}_r$. Here, the subscript g denotes the ground degrees of freedom and r denotes

the response degrees of freedom. Eq. (11) can be rearranged by separating the degrees of freedom into two groups as known and unknown (Abdel-Ghaffar and Stringfellow 1984).

$$\begin{bmatrix} M_{rr} & M_{rg} \\ M_{gr} & M_{gg} \end{bmatrix} \begin{Bmatrix} \ddot{v}_r \\ \ddot{v}_g \end{Bmatrix} + \begin{bmatrix} C_{rr} & C_{rg} \\ C_{gr} & C_{gg} \end{bmatrix} \begin{Bmatrix} \dot{v}_r \\ \dot{v}_g \end{Bmatrix} + \begin{bmatrix} K_{rr} & K_{rg} \\ K_{gr} & K_{gg} \end{bmatrix} \begin{Bmatrix} v_r \\ v_g \end{Bmatrix} = \begin{Bmatrix} 0 \\ 0 \end{Bmatrix} \tag{12}$$

It is possible to separate the total displacement vectors as quasi-static and dynamic components as follows

$$\begin{Bmatrix} v_r \\ v_g \end{Bmatrix} = \begin{Bmatrix} v_{sr} \\ v_{sg} \end{Bmatrix} + \begin{Bmatrix} v_{dr} \\ v_{dg} \end{Bmatrix} \tag{13}$$

where the subscript s denotes quasi-static component and d denotes dynamic component. Substituting of Eq. (13) into Eq. (12), the equation of motion of the dynamic component of the response degrees of freedom can be written as

$$[M_{rr}]\{\ddot{v}_{dr}\} + [C_{rr}]\{\dot{v}_{dr}\} + [K_{rr}]\{v_{dr}\} = \{F_{eff}\} \tag{14}$$

where $\{F_{eff}\}$ is the vector of effective forces acting on the response degrees of freedom and is equal to

$$\{F_{eff}\} = -[M_{rr} \;\; M_{rg}] \begin{Bmatrix} \ddot{v}_{sr} \\ \ddot{v}_{sg} \end{Bmatrix} - [C_{rr} \;\; C_{rg}] \begin{Bmatrix} \dot{v}_{sr} \\ \dot{v}_{sg} \end{Bmatrix} - [K_{rr} \;\; K_{rg}] \begin{Bmatrix} v_{sr} \\ v_{sg} \end{Bmatrix} \tag{15}$$

If all time-dependent terms are omitted from Eqs. (14) and (15), only the last term of Eq. (15) remains and this must be equal to zero. This means that

$$\{v_{sr}\} = -[K_{rr}]^{-1}[K_{rg}]\{v_{sg}\} = [R_{rg}]\{v_{sg}\} \tag{16}$$

where $[R_{rg}]$ is the ground displacement shape matrix, $\{v_{sr}\}$ is the quasi-static displacement. The damping contribution to the vector of effective forces can be expected to be small and therefore, it is frequently neglected regardless of the type of damping involved (Clough and Penzien 1993). If the effective force expression is arranged by using Eqs. (16) and (14), the equation of motion of the dynamic components, $\{v_{dr}\}$, of the response degrees of freedom can be written as

$$[M_{rr}]\{\ddot{v}_{dr}\} + [C_{rr}]\{\dot{v}_{dr}\} + [K_{rr}]\{v_{dr}\} = -[M_{rr}][R_{rg}]\{\ddot{v}_{sg}\} \tag{17}$$

The equations of motion of an isolated bridge subjected to spatially varying earthquake ground motion can be expressed as

$$[M_{rr}]\{\ddot{v}_{dr}\} + [C_{rr}]\{\dot{v}_{dr}\} + [K_{rr}]\{v_{dr}\} = -[M_{rr}][R_{rg}]\{\ddot{v}_{sg} + \ddot{v}_b\} \tag{18}$$

$$m_b\ddot{v}_b + c_b\dot{v}_b + \mu_e W \mathrm{sgn}(\dot{v}_b) + k_b v_b = -m_b\ddot{v}_{sg} \tag{19}$$

where m_b, c_b and k_b are mass, damping and stiffness of the base isolation system; $\ddot{v}_b, \dot{v}_b$ and v_b are acceleration, velocity and displacement of the DCFP; μ_e is the effective coefficient of friction on the concave surfaces of the DCFP and W is the total weight carried by the DCFP. Eq. (19) then is a non-linear differential equation due to the presence of friction. This non-linear governing equation of motion can be written in a corresponding equivalent linearized form as Jangid and Banerji (1998)

$$m_b\ddot{v}_b + c_b\dot{v}_b + k_b v_b = -m_b\ddot{v}_{sg} \tag{20}$$

where c_e is an equivalent damping constant that is obtained by minimizing the mean square of the difference between Eqs. (19) and (20), given by

$$c_e = c_b + \sqrt{\frac{2}{\pi}}\frac{\mu_e W}{\sigma_{\dot{v}_b}} \tag{21}$$

where $\sigma_{\dot{v}_b}$ is the root mean square value of velocity of the DCFP and c_b is the damping constant of the DCFP. It should be noted that the non-linear behaviour of the DCFP still exists in Eq. (20) due to the dependence of c_e on the root mean square value of velocity of the DCFP. This analysis procedure is well known as equivalent linearization technique in non-linear stochastic analysis. It can be shown that the mean square relative velocity of isolation systems can be expressed as (Jangid and Banerji 1998, Constantinou and Papageorgiou 1990)

$$\sigma_{\dot{v}_b} = \frac{\mu_e g}{2\sqrt{2\pi}\xi_b\omega_b}\left(\sqrt{1 + \frac{4\pi^2\xi_b S_{\ddot{y}_g}(\omega_b)}{\mu_e^2 g^2}} - 1\right) \tag{22}$$

where ξ_b and ω_b are natural frequency and damping ratio of isolation system; $S_{\ddot{y}_g}$ is the power spectral density function of the ground motion.

5. Stochastic response

The variance of the ith total response for the spatially varying ground motion is expressed as Ates *et al*. (2006)

$$\sigma_{z_i}^2 = \sigma_{z_i}^{2qs} + \sigma_{z_i}^{2d} + 2\mathrm{Cov}(z_i^{qs}, z_i^d) \tag{23}$$

in which $\sigma_{z_i}^{2qs}$ is the variance of the ith quasi-static response component; $\sigma_{z_i}^{2d}$ is the variance of the ith dynamic response component and $\mathrm{Cov}(z_i^{qs}, z_i^d)$ is the covariance between the ith quasi-static and dynamic components. The variance of the ith quasi-static component can be written as

$$\sigma_{z_i}^{2qs} = \int_{-\infty}^{\infty} S_{z_i}^{qs}(\omega)d\omega = \sum_{\ell=1}^{r}\sum_{m=1}^{r} A_{i\ell}A_{im}\int_{-\infty}^{\infty}\frac{1}{\omega^4}S_{\ddot{y}_{g_\ell}\ddot{y}_{g_m}}(\omega)d\omega \tag{24}$$

in which $S_{z_i}^{qs}(\omega)$ is the ith quasi-static component of the spectral density function of the structural response; r is the number of restrained degrees of freedom; $S_{\ddot{y}_{g_\ell}\ddot{y}_{g_m}}(\omega)$ is the cross-spectral density function of accelerations between supports ℓ and m; and $A_{i\ell}$ and A_{im} are equal to static displacements for unit displacements assigned to each support points. The variance of the ith dynamic response component may be defined as

$$\sigma_{z_i}^{2d} = \int_{-\infty}^{\infty} S_{z_i}^{d}(\omega)d\omega = \sum_{j=1}^{n}\sum_{k=1}^{n}\sum_{\ell=1}^{r}\sum_{m=1}^{r}\psi_{ij}\psi_{ik}\Gamma_{\ell j}\Gamma_{mk}\int_{-\infty}^{\infty}H_j(-\omega)H_k(\omega)S_{\ddot{y}_{g_\ell}\ddot{y}_{g_m}}(\omega)d\omega \tag{25}$$

where $S_{z_i}^{qs}(\omega)$ is the ith dynamic component of the spectral density function of the structural response; $H(\omega)$ is the frequency response function; n is the number of free degrees of freedom; ψ

is the eigenvectors; and Γ is the modal participation factor. The covariance of the ith quasi-static and dynamic components is obtained as

$$\mathrm{Cov}(z_i^{qs}, z_i^d) = -\sum_{j=1}^{n}\sum_{\ell=1}^{r}\sum_{m=1}^{r}\psi_{ij}A_{i\ell}\Gamma_{mj}\left(\int_{-\infty}^{\infty}\frac{1}{\omega^2}H_j(\omega)S_{\ddot{v}_{g_\ell}\ddot{v}_{g_m}}(\omega)d\omega\right) \tag{26}$$

5.1 Expected maximum value

The expected maximum value is considered to be the most important parameter in the stochastic analysis of structures affected by seismic loads. This value is the mean value of all maximum values. The expected maximum value depending on the peak factor and the root-mean-square response can be expressed as

$$E = p\sqrt{\lambda_0} \tag{27}$$

Standard deviation of the expected maximum value is expressed as

$$\sigma = \frac{q}{p}E \tag{28}$$

where λ_0 is the zeroth spectral moment, p and q are the peak factors, the functions of the duration of the motion and the mean zero crossing rate, respectively (Der Kiureghian 1980).

Frequency of occurrence is described as the average number of times that the line ($y(t) = 0$) is crossed by the response in a unit of time. For Gaussian process of zero average, the average number of times in the zero level crossed by the process in a unit of time is expressed as

$$\nu = \frac{1}{\pi}\sqrt{\frac{\lambda_2}{\lambda_0}} \tag{29}$$

where λ_2 is the second spectral moment The spectral moments can be expressed in terms of power spectral density function and frequency (Akkose *et al.* 2007, Dumanoglu and Sever 1990). Because the zero level is crossed two times for each cycle, frequency of occurrence for the response process will be equal to $\nu/2$ and defined by Eq. (29).

5.2 Spatially varying earthquake ground motion model

Because of the complex nature of the earth crust, earthquake ground motions will not be the same at distances of the dimensions of long span structures, such as bridges. It is obvious that because of travelling with finite velocity, coherency loss due to reflections and refractions and difference of local soil conditions at the supports, earthquake ground motions will be subjected to significant variation at the support points of the bridge. This variation causes internal forces due to quasi-static displacements. In the case of uniform ground motions, quasi-static displacements normally do not produce internal forces. Therefore, while analysing large structures, spatially varying earthquake ground motions should be considered and total displacements have to be used in expressing the governing equation of motion. The spatially varying earthquake ground motion includes incoherence, wave-passage and site-response effects. The wave-passage effect results from differences in the arrival times of waves at support points. The incoherence effect results from the reflections and refractions of seismic waves through the soil during their propagation. The site-

response effect results from differences in local soil conditions at the support point. These effects are characterised by the coherency function in frequency domain.

The cross-spectral density function of the earthquake ground motion, between support points ℓ and m is expressed as Harichandran and Wang (1988)

$$S_{\ddot{v}_{g_\ell}\ddot{v}_{g_m}}(\omega) = \gamma_{\ell m}(\omega)\sqrt{S_{\ddot{v}_{g_\ell}\ddot{v}_{g_\ell}}(\omega)S_{\ddot{v}_{g_m}\ddot{v}_{g_m}}(\omega)} \tag{30}$$

where $\gamma_{\ell m}(\omega)$ denotes the coherency function. The power spectral density function is assumed to be of the following form modified by Clough and Penzien (1993)

$$S_{\ddot{v}_g}(\omega) = S_o\frac{\omega_f^4 + 4\xi_f^2\omega_f^2\omega^2}{(\omega_f^2-\omega^2)^2 + 4\xi_f^2\omega_f^2\omega^2}\frac{\omega^4}{(\omega_g^2-\omega^2)^2 + 4\xi_g^2\omega_g^2\omega^2} \tag{31}$$

where S_o is the amplitude of the white-noise process; ω_f and ξ_f are the resonant frequency and damping of the first filter, and ω_g and ξ_g are those quantities of the second filter.

In this paper, S_o is obtained for each soil type by equating the variance of the ground acceleration to the variance of the east-west component of Erzincan, Turkey, earthquake in 1992. The calculated values of the intensity parameter for each soil type are shown in Table 1. Homogeneous soft, medium and firm soil types (Fig. 3) are used for the non-isolated and isolated bridge supports and the filter parameters proposed Der Kiureghian and Neuenhofer (1991) are utilised as shown in Table 1.

The dimensionless complex coherency function is defined as Der Kiureghian (1996), Nakamura *et al.* (1993)

$$\gamma_{\ell m}(\omega) = |\gamma_{\ell m}(\omega)|^i\gamma_{\ell m}(\omega)^w\gamma_{\ell m}(\omega)^s \tag{32}$$

where $|\gamma_{\ell m}(\omega)|^i$ characterises the incoherence effect, $\gamma_{\ell m}(\omega)^w$ indicates the complex valued wave-

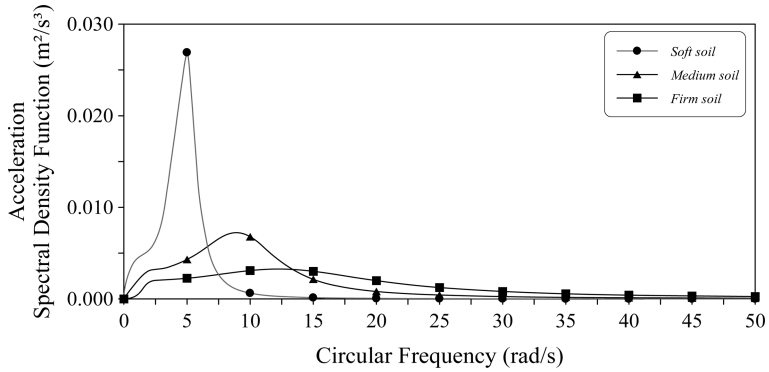

Fig. 3 Acceleration spectral density function for different soil conditions

Table 1 Filter and intensity parameter of filtered white-noise process for different soil types

Soil type	ω_f (rad/s)	ξ_f	ω_g (rad/s)	ξ_g	S_0 (m^2/s^3)
Firm	15.0	0.6	1.5	0.6	0.00177
Medium	10.0	0.4	1.0	0.6	0.00263
Soft	5.0	0.2	0.5	0.6	0.00369

passage effect and $\gamma_{\ell m}(\omega)^s$ denotes the complex valued site-response effect.

For the incoherence effect, resulting from reflections and refractions of waves through the soil during their propagation, an extensively used model is considered. The model proposed by Harichandran and Vanmarcke (1986) is defined as

$$|\gamma_{\ell m}(\omega)|^i = A\exp\left[-\frac{2d_{\ell m}}{\alpha\theta(\omega)}(1-A+\alpha A)\right]+(1-A)\exp\left[-\frac{2d_{\ell m}}{\theta(\omega)}(1-A+\alpha A)\right] \tag{33}$$

$$\theta(\omega) = k\left[1+\left(\frac{\omega}{2\pi f_o}\right)^b\right]^{-1/2} \tag{34}$$

where $d_{\ell m}$ is the distance between support points ℓ and m; A, α, k, f_o and b are 0.636, 0.0186, 31200, 1.51 Hz and 2.95, respectively (Zerva 1991, Dumanoglu and Soyluk 2002).

The wave-passage effect resulting from the difference in the arrival times of waves at support points is defined as Der Kiureghian (1996), Nakamura *et al.* (1993)

$$\gamma_{\ell m}(\omega)^w = e^{i(-\omega d^L_{\ell m}/v_{app})} \tag{35}$$

where v_{app} is the apparent wave velocity and $d^L_{\ell m}$ is the projection of $d_{\ell m}$ on the ground surface along the direction of propagation of seismic waves. The apparent wave velocities employed in this study are selected as 300, 600 and 1200 m/s for soft, medium and firm soil types, respectively.

The site-response effect due to the differences in the local soil conditions is obtained as Der Kiureghian (1996), Nakamura *et al.* (1993)

$$\gamma_{\ell m}(\omega)^s = e^{i(\tan^{-1}(\mathrm{Im}[H_\ell(\omega)H_m(-\omega)]/\mathrm{Re}[H_\ell(\omega)H_m(-\omega)])} \tag{36}$$

where $H_\ell(\omega)$ is the local soil frequency response function representing the filtration through the soil layers.

7. Numerical computations

Stochastic analysis of the isolated and non-isolated Jindo Bridge model is performed for the spatially varying ground motion by taking into account the incoherence and wave-passage effects. For the soil condition where the bridge supports are located, three different soil condition sets are considered. All the supports are assumed to be founded on soft, medium and firm soil conditions. Fig. 4 defines the 2D mathematical model of the Jindo Bridge with the details indicating the places where the DCFP bearings are placed. The spatially varying earthquake ground motion is applied to the bridge in the vertical direction. Fig. 5 shows the bridge system founded on different soil conditions for vertically applied ground motions. The vertical input motion is assumed to travel across the bridge from Jindo Island side to mainland side with finite velocities of 300 m/s, 600 m/s and 1200 m/s for soft, medium and firm soil conditions, respectively. The analyses are carried out with a recently developed computer code SVEM (Dumanoglu and Soyluk 2002), which is modified to include the sliding bearing behaviour. In this study, total responses obtained at the deck and towers are compared for isolated and non-isolated bridge models when subjected to the spatially varying ground motions. Three different homogeneous soil conditions are also used herein for comparison purposes.

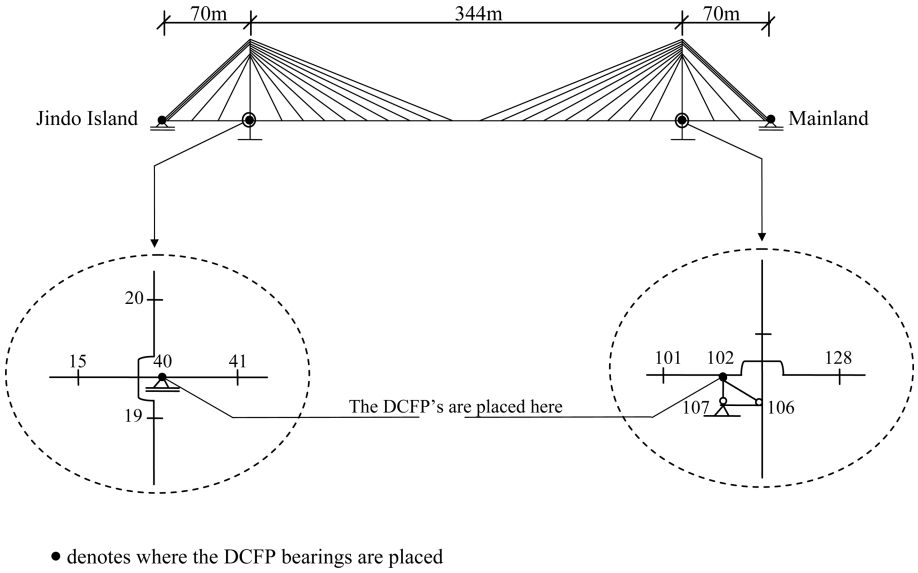

Fig. 4 2D Mathematical Modelling of the Jindo Bridge

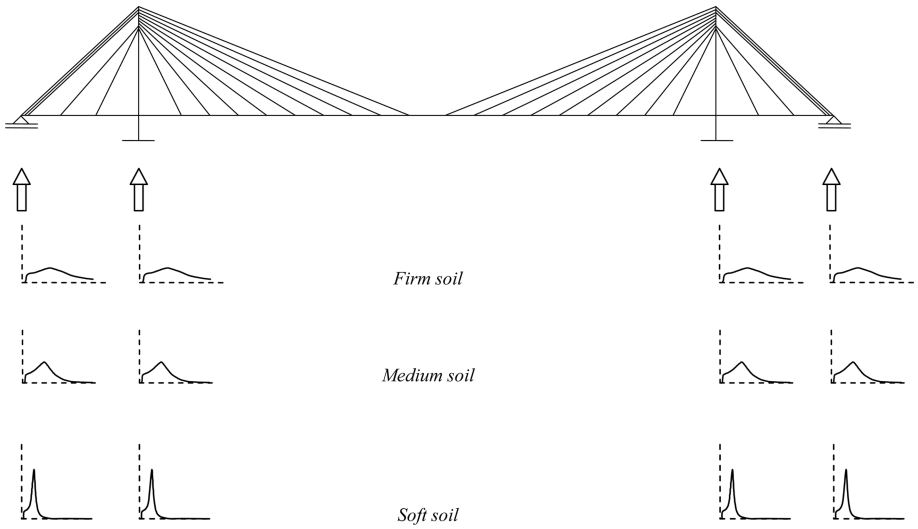

Fig. 5 The Bridge subjected to spatially varying ground motions for different soil conditions

8. Numerical results

8.1 Mean of maximum deck responses

Eq. (27) is used to calculate the mean of maximum response values of the considered bridge system. Figs. 6-8 give the mean of maximum total deck bending moments for the isolated and non-isolated cable-stayed bridge models founded on firm, medium and soft soil conditions, respectively. Mean of maximum bending moments obtained for the isolated bridge system are considerably

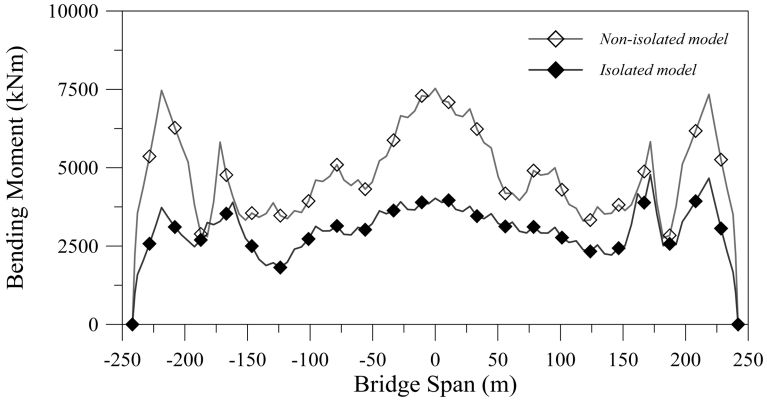

Fig. 6 Mean of maximum total deck bending moments (firm soil)

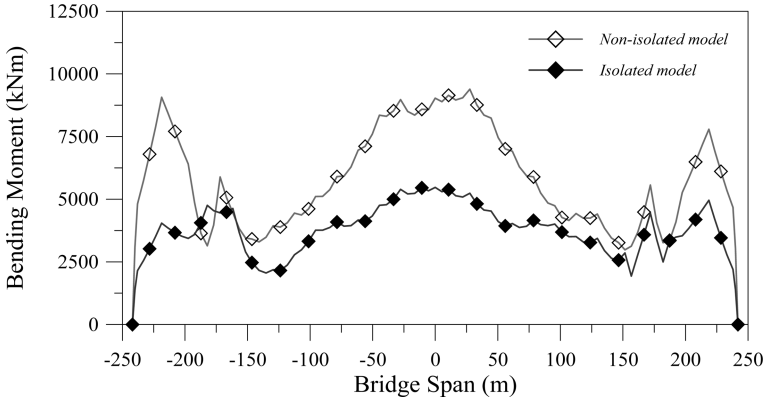

Fig. 7 Mean of maximum total deck bending moments (medium soil)

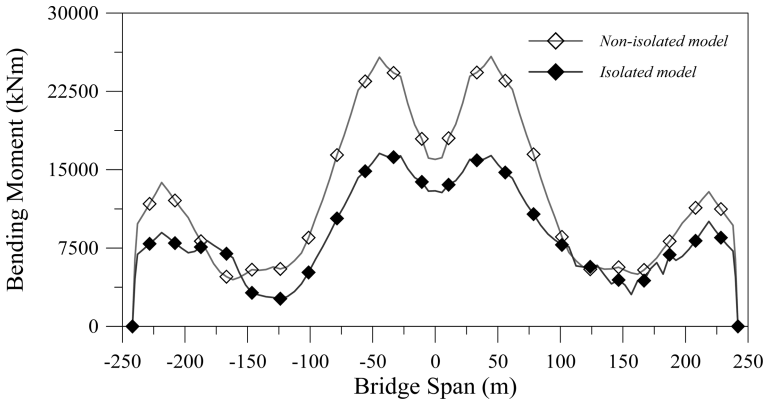

Fig. 8 Mean of maximum total deck bending moments (soft soil)

smaller than the mean of maximum responses obtained for the non-isolated bridge system. The deck bending moments obtained from the stochastic analysis of the isolated bridge model are decreased around 30-55% if compared with the results obtained for the non-isolated bridge model. Depending on the homogeneous soil conditions, while largest bending moments are obtained for the soft soil

condition case, smallest bending moments are obtained for the firm soil condition case. Homogeneous medium soil condition case results bending moments between the results obtained for the firm and soft soil condition cases. For the isolated and non-isolated bridge models, the incoherence and wave-passage effects are considered for the spatially varying ground motion. The results clearly show that consideration of double concave friction pendulum bearings for the isolation of the cable-stayed bridge system for the stochastic earthquake response analysis when the bridge system is subjected to the spatially varying earthquake ground motion decreases the deck bending moments.

The mean of maximum total deck axial forces for the isolated and non-isolated cable-stayed bridge models are given Figs. 9-11. The reduction of the deck axial forces obtained for the isolated model is obvious, if the axial forces are compared with those obtained for the non-isolated bridge model. Significant reduction of the axial forces is provided at the connection points between the deck and towers. The reduction obtained for the homogeneous firm, medium and soft soil conditions are about 56%, 55% and 28%, respectively. However, at the nodal points located at the middle of the deck, the axial forces obtained for the isolated and non-isolated bridge models are very close to each other.

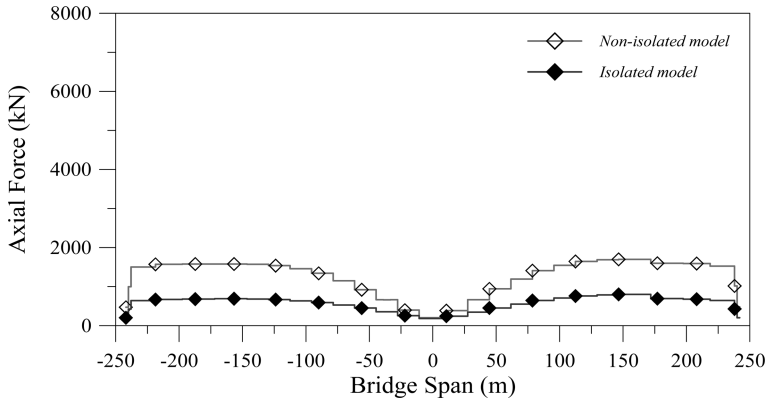

Fig. 9 Mean of maximum total deck axial forces (firm soil)

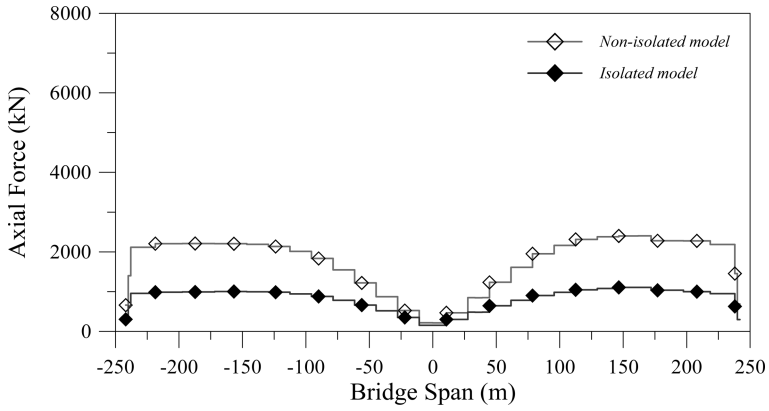

Fig. 10 Mean of maximum total deck axial forces (medium soil)

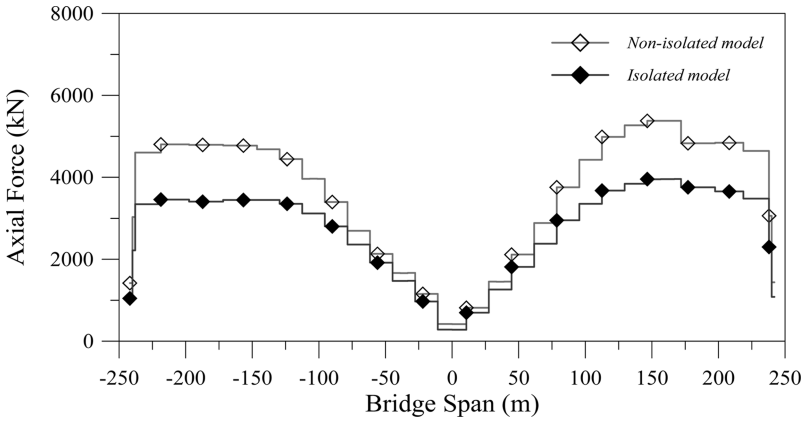

Fig. 11 Mean of maximum total deck axial forces (soft soil)

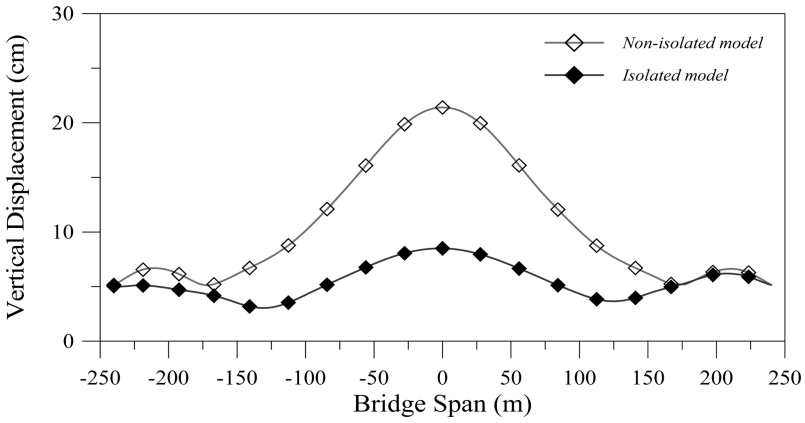

Fig. 12 Mean of maximum total deck displacements (firm soil)

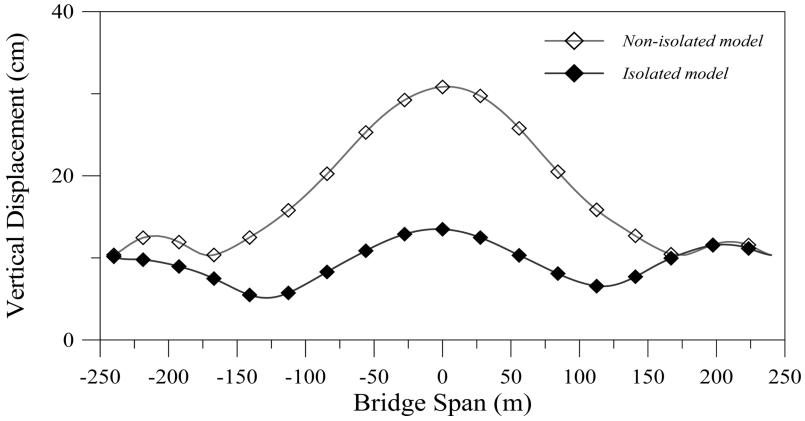

Fig. 13 Mean of maximum total deck displacements (medium soil)

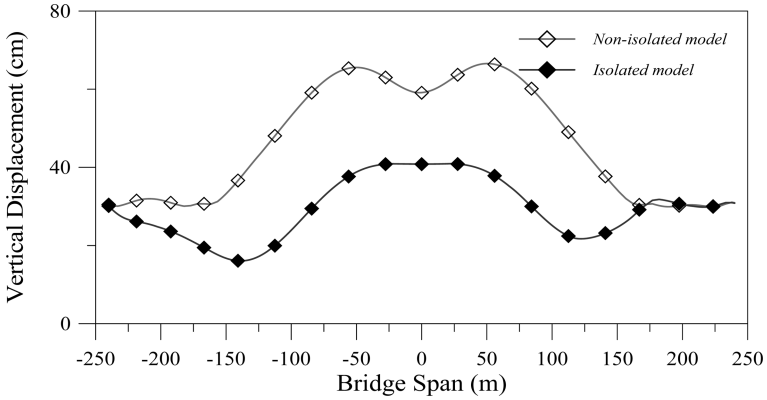

Fig. 14 Mean of maximum total deck displacements (soft soil)

The mean of maximum total vertical deck displacements for the isolated and non-isolated cable-stayed bridge models are compared in Figs. 12-14. The vertical displacements of the deck are considerably decreased for the isolated system due to the DCFP bearings while all the supports of the bridge are assumed to be founded on firm, medium and soft soil conditions, respectively. Depending on the local soil conditions the vertical displacements obtained at the middle of the deck for the isolated system causes 60%, 56% and 31% smaller responses than those of the non-isolated system for firm, medium and soft soil conditions, respectively.

8.2 Mean of maximum tower responses

The mean of maximum total bending moments, shear forces and axial forces obtained at the mainland tower of the isolated and non-isolated cable-stayed bridge systems are compared in Figs. 15-23. It is obvious that the member forces obtained for the isolated bridge system are, as expected, significantly decreased by using the DCFP bearings, relative to the member forces obtained for the non-isolated bridge model. Depending on the local soil conditions, while the largest member forces are obtained at the soft soil conditions case, the smallest member forces are obtained at the firm soil condition case. Although the decrement ratio obtained for each member force along

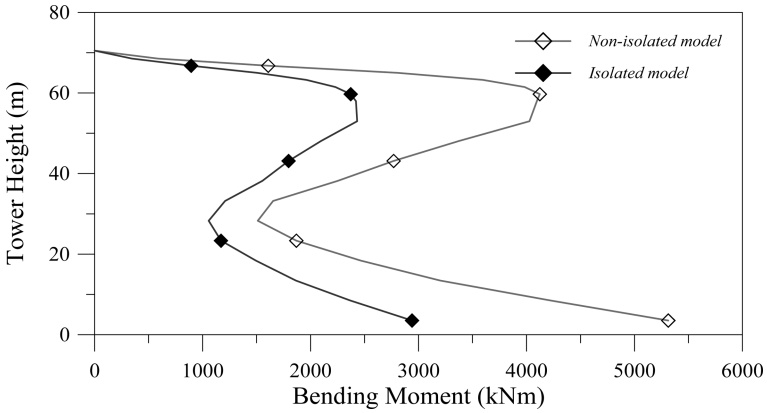

Fig. 15 Mean of maximum total bending moments of the mainland tower (firm soil)

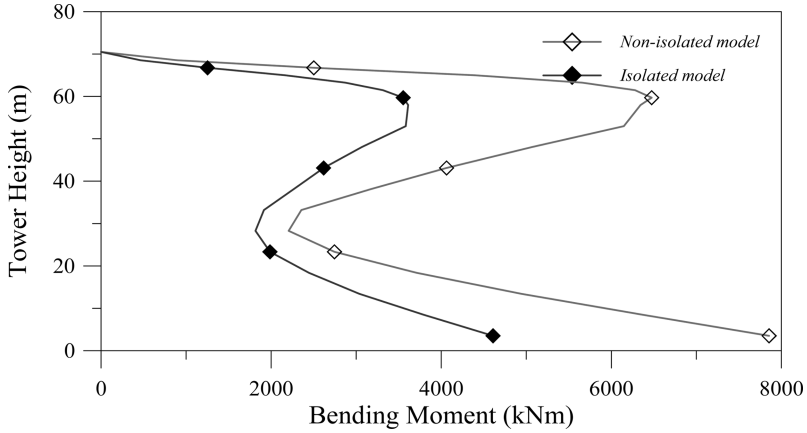

Fig. 16 Mean of maximum total bending moments of the mainland tower (medium soil)

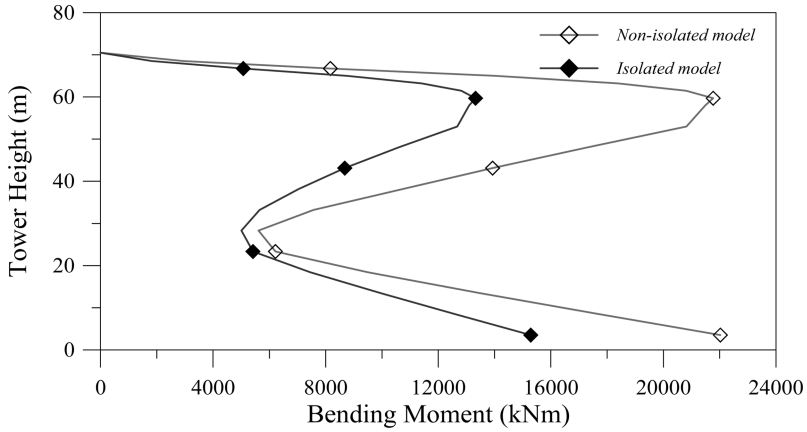

Fig. 17 Mean of maximum total bending moments of the mainland tower (soft soil)

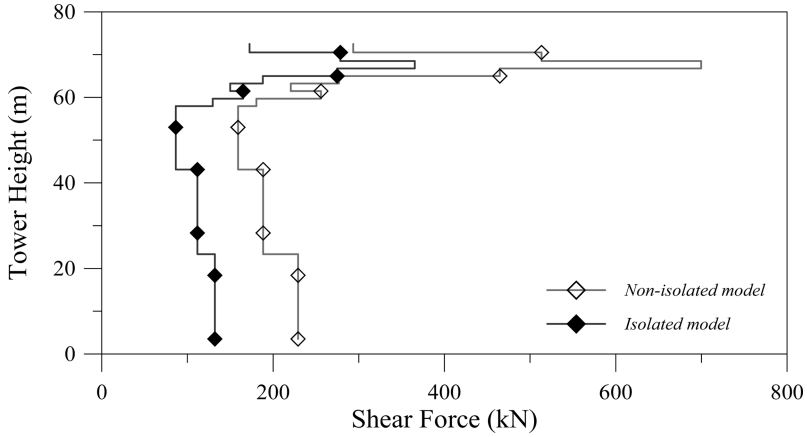

Fig. 18 Mean of maximum total shear forces of the mainland tower (soft soil)

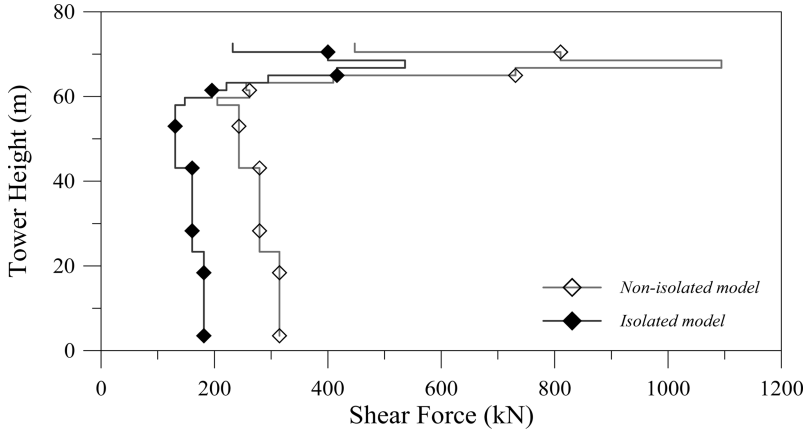

Fig. 19 Mean of maximum total shear forces of the mainland tower (medium soil)

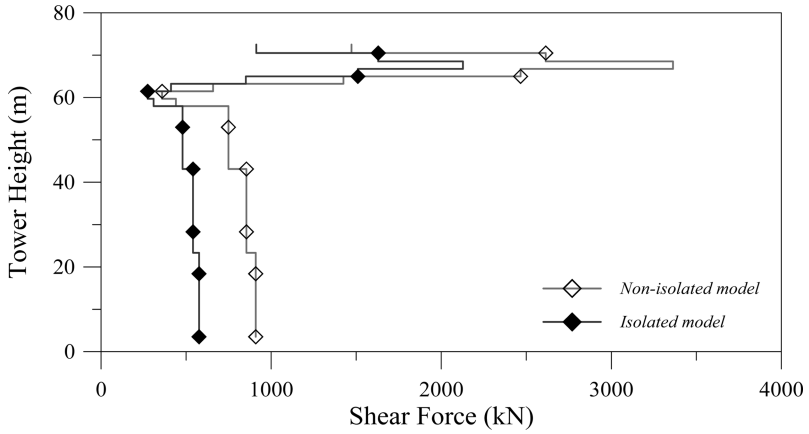

Fig. 20 Mean of maximum total shear forces of the mainland tower (soft soil)

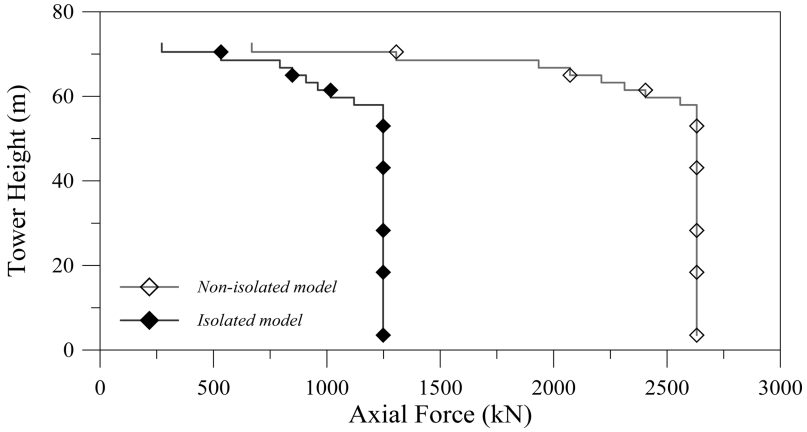

Fig. 21 Mean of maximum total axial forces of the mainland tower (soft soil)

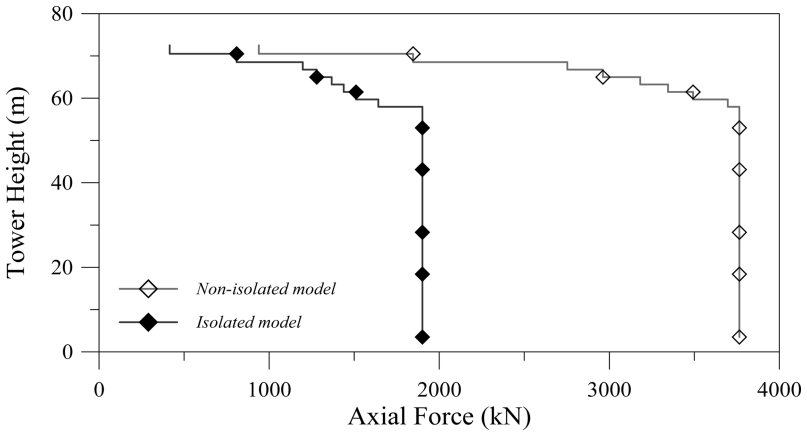

Fig. 22 Mean of maximum total axial forces of the mainland tower (medium soil)

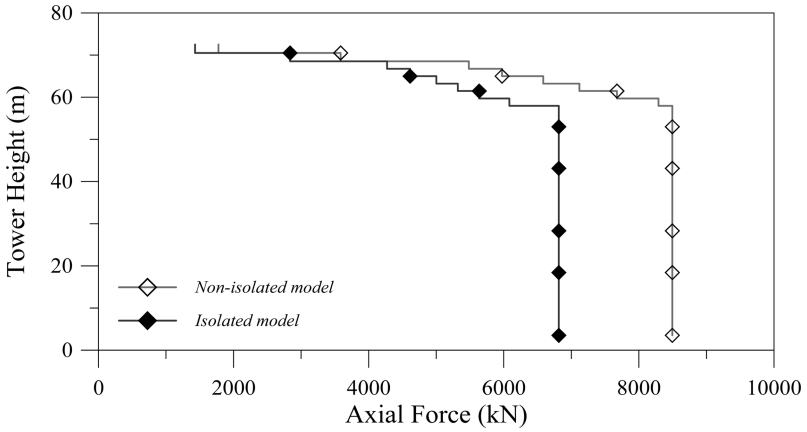

Fig. 23 Mean of maximum total axial forces of the mainland tower (soft soil)

the height of the isolated bridge tower is arbitrarily changing, the maximum decrement ratio obtained for the member forces fluctuates around 37%, 39% and 43% for the bending moment, shear force and axial force, respectively. Because the variations obtained for the Jindo Island tower member forces are very similar, those results are not reported in this paper.

The variation obtained for the Jindo Island tower horizontal displacements is different from the variation obtained for the member forces of the isolated and non-isolated systems (Figs. 24-26). For the homogeneous firm soil condition case the horizontal displacements for the isolated system are larger than the displacements of the non-isolated system along the height of the tower after 30 m. The horizontal displacement at the top of the tower obtained for the isolated system is 24% smaller than the displacement obtained for the non-isolated system. Similar variation is also obtained for the homogeneous medium soil condition case. Isolated bridge system yields larger displacements after 40 m along the height of the tower. At the top of the tower the difference between the isolated and non-isolated tower displacements is 11%. The variation obtained for the soft soil condition case is quite different. The horizontal displacements obtained for the non-isolated system are larger than those of the displacements obtained for the isolated system. The difference between the responses of the isolated and non-isolated systems at the top of the tower is calculated as 12%.

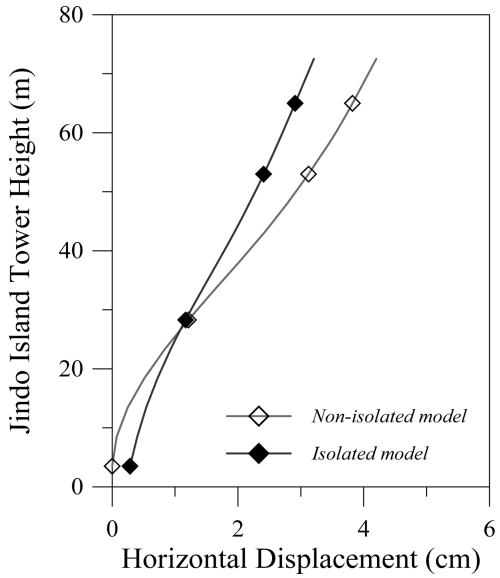

Fig. 24 Mean of maximum total displacements of the Jindo Island tower (firm soil)

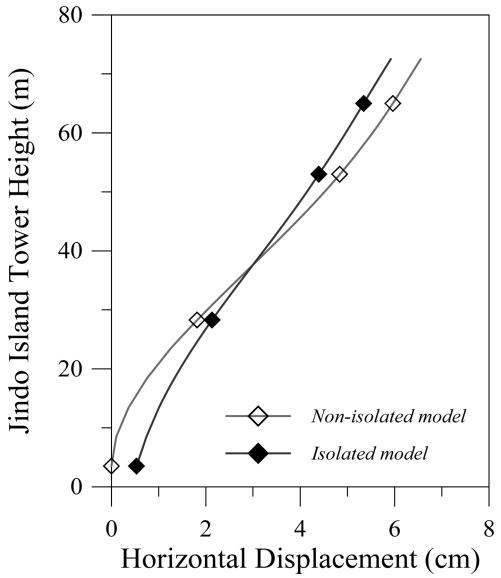

Fig. 25 Mean of maximum total displacements of the Jindo Island tower (medium soil)

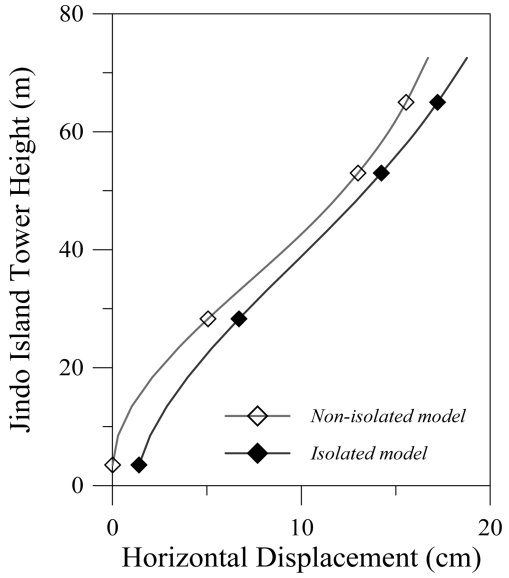

Fig. 26 Mean of maximum total displacements of the Jindo Island tower (soft soil)

8.3 Frequency of occurrence

Frequencies of occurrences of mean of maximum total deck bending moments are calculated by Eq. (29) and presented in Figs. 27-29 for firm, medium and soft soil conditions, respectively. For firm soil condition case, the frequencies of occurrences of mean of maximum total deck bending moments at the mid-span for the isolated and non-isolated systems are 1.32 Hz and 0.98 Hz,

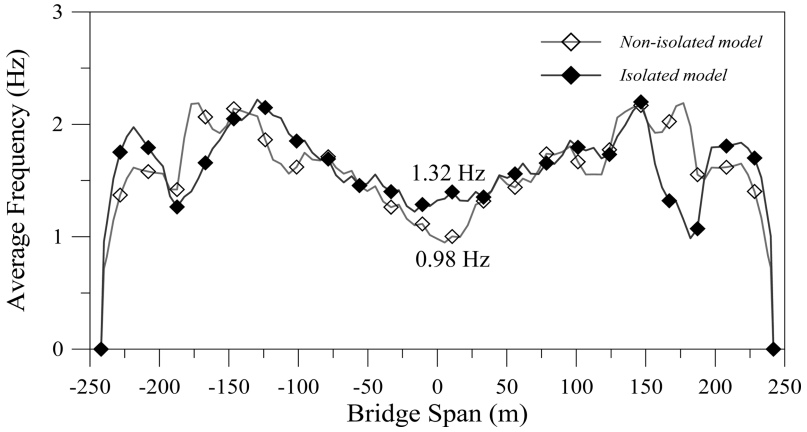

Fig. 27 Average frequencies of occurrence of mean of maximum total deck bending moments (firm soil)

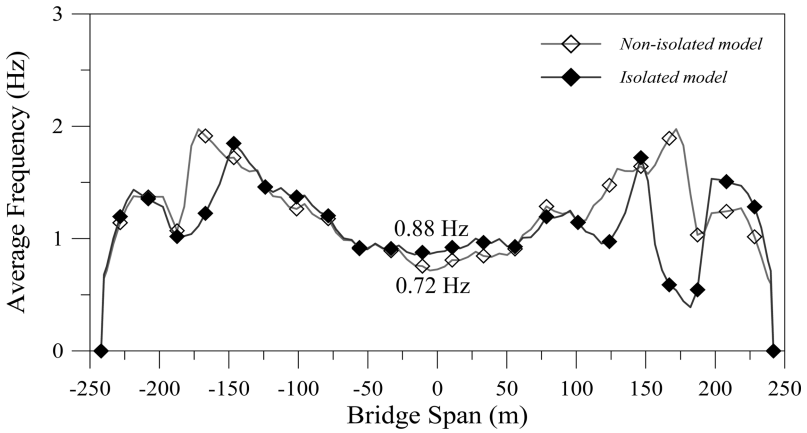

Fig. 28 Average frequencies of occurrence of mean of maximum total deck bending moments (medium soil)

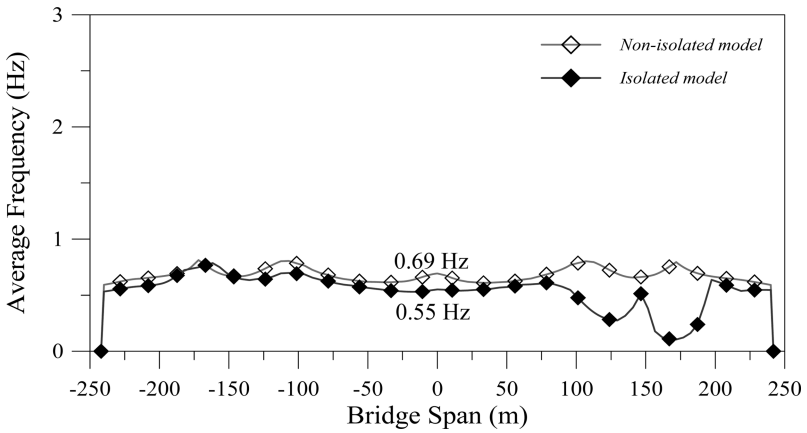

Fig. 29 Average frequencies of occurrence of mean of maximum total deck bending moments (soft soil)

respectively. The frequencies of occurrences are decreasing for the medium and soft soil conditions.

9. Conclusions

This study outlines an investigation about the stochastic responses of isolated and non-isolated cable-stayed bridge systems subjected to spatially varying ground motions. For the isolated bridge system, double concave friction pendulum bearings are placed between the deck and the towers as base isolation devices. Filtered white noise ground motion is considered to model the earthquake ground motion. The incoherence and the wave-passage effects are taken into account for the spatially varying earthquake ground motion. The analyses are carried out for the isolated and non-isolated bridges, separately. The mean of maximum response values of the isolated and non-isolated bridge systems are compared with each other for different homogeneous soil condition cases. The results obtained from this study can be categorized as:

(i) It is clear that depending on the type of local soil conditions the total response values decrease from homogeneous firm soil to the soft soil condition case.
(ii) The mean of maximum deck member forces are considerably decreased (30-50%) due to the DCFP bearings while all the supports of the bridge are assumed to be founded on homogeneous firm, medium and soft soil conditions.
(iii) Important reductions are also observed for the vertical deck displacements of the isolated bridge system. The maximum reduction is reported at the middle of the deck as 60% forfirm soil condition case.
(iv) The member forces obtained at the mainland tower of the isolated bridge system are significantly decreased by using the DCFP bearings, relative to the member forces obtained for the non-isolated bridge model. The maximum decrement ratio obtained for the member forces fluctuates around 37%, 39% and 43% for the bending moment, shear force and axial force, respectively.
(v) Although the variations obtained for the mean of maximum horizontal tower displacements at the isolated and non-isolated systems show similarity to the member force responses, depending on the soil conditions the horizontal tower displacements of the isolated bridge system can be smaller than the displacement responses obtained at the non-isolated bridge system.
(vi) Depending on the local soil conditions at the support points of the bridge system, significant changes are reported for the frequencies of occurrences of the mean of maximum response values of the isolated and non-isolated bridge systems. The frequencies of occurrences are decreasing by changing the soil conditions from firm soil condition to soft soil condition at the support points.

References

Abdel-Ghaffar, A.M. and Stringfellow, R.G. (1984), "Response of suspension bridges to travelling earthquake excitations, Part I-II", *Soil Dyn. Earthq. Eng.*, **3**, 62-81.

Akkose, M., Adanur, S., Bayraktar, A. and Dumanoglu, A.A. (2007), "Stochastic seismic response of Keban Dam by finite element method", *Appl. Math. Comput.*, **184**, 704-714.

Ali, H.M. and Abdel-Ghaffar, A.M. (1994), "Seismic energy dissipation for cable-stayed bridges using passive devices", *Earthq. Eng. Struct. Dyn.*, **23**, 877-893.
Ates, S., Bayraktar, A. and Dumanoglu, A.A. (2006), "The effect of spatially varying earthquake ground motions on the stochastic response of bridges isolated with friction pendulum systems", *Soil Dyn. Earthq. Eng.*, **26**, 31-44.
Ates, S., Dumanoglu, A.A. and Bayraktar, A. (2005), "Stochastic response of seismically isolated highway bridges with friction pendulum systems to spatially varying earthquake ground motions", *Eng. Struct.*, **27**, 1843-1858.
Betti, R., Abdel-Ghaffar, A.M. and Niazy, A.S. (1993), "Kinematic soil-structure interaction for long-span cable-supported bridges", *Earthq. Eng. Struct. Dyn.*, **22**, 415-430.
Clough, R.W. and Penzien, J. (1993), *Dynamics of Structures*, 2nd ed. Singapore: McGraw Hill, Inc.
Constantinou, M.C. (2004), "Friction pendulum double concave bearing", NEES Report, available at: http://nees.buffalo.edu/dec304/FP-DC%20Report-DEMO.pdf.
Constantinou, M.C. and Papageorgiou, A.S. (1990), "Stochastic response of practical sliding isolation systems", *Probabilist. Eng. Mech.*, **5**, 27-34.
Der Kiureghian, A. (1980), "Probabilistic modal combination for earthquake loading", in: Proceeding of Seventh World Conference on Earthquake Engineering, Istanbul, 729-736.
Der Kiureghian, A. (1996), "A coherency model for spatially varying ground motions", *Earthq. Eng. Struct. Dyn.*, **25**, 99-111.
Der Kiureghian, A. and Neuenhofer, A. (1991), "A response spectrum method for multiple-support seismic excitations", In: Report No. UCB/EERC-91/08. Berkeley (CA): Earthquake Engineering Research Center, College of Engineering, University of California.
Dumanoglu, A.A. and Sever, R.T. (1990), "Stochastic response of suspension bridges to earthquake forces", *Earthq. Eng. Struct. Dyn.*, **19**, 133-152.
Dumanoglu, A.A. and Soyluk, K. (2002), "SVEM: A stochastic structural analysis program for spatially varying earthquake motions", Turkish Earthquake Foundation, TDV/KT 023-76.
Fenz, D.M. and Constantinou, M.C. (2006), "Behaviour of double concave Friction Pendulum bearing", *Earthq. Eng. Struct. Dyn.*, **35**, 1403-1424.
Fleming, J.F. and Egeseli, E.A. (1980), "Dynamic behaviour of a cable-stayed bridge", *Earthq. Eng. Struct. Dyn.*, **8**, 1-16.
Garevski, M., Dumanoglu, A.A. and Severn, R.T. (1988), "Dynamic characteristics and seismic behaviour of Jindo Bridge, South Korea", *Struct. Eng. Rev.,* **1**, 141-149.
Harichandran, R.S. and Vanmarcke, E.H. (1986), "Stochastic variation of earthquake ground motion in space and time", *J. Eng. Mech.*, **112**, 154-174.
Harichandran, R.S. and Wang, W. (1988), "Response of one- and two-span beams to spatially varying seismic excitation", In: Report to the National Science Foundation MSU-ENGR-88-002. Michigan (MI): Department of Civil and Environmental Engineering, College of Engineering, Michigan State University.
Harichandran, R.S., Hawwari, A. and Sweidan, B.N. (1996), "Response of long-span bridges to spatially varying ground motion", *J. Struct. Eng.*, **122**, 476-484.
Hyakuda, T., Saito, K., Matsushita, T., Tanaka, N., Yoneki, S., Yasuda, M., Miyazaki, M., Suzuki, A. and Sawada, T. (2001), "The structural design and earthquake observation of a seismic isolation building using Friction Pendulum system", Proceedings, 7th International Seminar on Seismic Isolation, Passive Energy Dissipation and Active Control of Vibrations of Structures, Assisi, Italy.
Jangid, R.S. and Banerji, P. (1998), "Effect of isolation damping on stochastic response of structures with nonlinear base isolators", *Earthq. Spectra.*, **14**, 95-114.
Jung, H. and Park, K. (2004), "Spencer Jr BF, Lee I. Hybrid seismic protection of cablestayed bridges", *Earthq. Eng. Struct. Dyn.*, **33**, 795-820.
Lou, L. and Zerva, A. (2005), "Effects of spatially variable ground motions on the seismic response of a skewed, multi-span, RC highway bridge", *Soil Dyn. Earthq. Eng.*, **25**, 729-740.
Morris, N.F. (1974), "Dynamic analysis of cable-stiffened structures", *J. Struct. Eng. Div.*, ASCE, **100**, 971-981.
Nakamura, Y., Der Kiureghian, A. and Liu, D. (1993), "Multiple-support response spectrum analysis of the Golden Gate Bridge", In: Report No. UCB/EERC-93/05. Berkeley (CA): Earthquake Engineering Research

Center, College of Engineering, University of California.
Nazmy, A.S. and Abdel-Ghaffar, A.M. (1987), "Seismic response analysis of cable stayed bridges subjected to uniform and multiple-support excitations", In: Report No. 87-SM-1. Princeton (NJ): Department of Civil Engineering, Princeton University.
Nazmy, A.S. and Abdel-Ghaffar, A.M. (1990), "Non-linear earthquake-response analysis of long-span cable-stayed bridges: Applications", *Earthq. Eng. Struct. Dyn.*, **19**, 63-76.
Nazmy, A.S. and Abdel-Ghaffar, A.M. (1990), "Non-linear earthquake-response analysis of long-span cable-stayed bridges: Theory", *Earthq. Eng. Struct. Dyn.*, **19**, 45-62.
Nazmy, A.S. and Abdel-Ghaffar, A.M. (1992), "Effects of ground motion spatial variability on the response of cable-stayed bridges", *Earthq. Eng. Struct. Dyn.*, **21**, 1-20.
Perotti, F. (1990), "Structural response to nonstationary multiple-support random excitation", *Earthq. Eng. Struct. Dyn.*, **19**, 513-527.
Soneji, B.B. and Jangid, R.S. (2006), "Effectiveness of seismic isolation for cable-stayed bridges", *Int. J. Struct. Stab. Dyn.*, **6**, 1-20.
Soneji, B.B. and Jangid, R.S. (2006), "Seismic control of cable-stayed bridge using semi-active hybrid system", *Bridge Struct.*, **2**, 45-60.
Soneji, B.B. and Jangid, R.S. (2007), "Passive hybrid systems for earthquake protection of cable-stayed bridge", *Eng. Struct.*, **29**, 57-70.
Soyluk, K. and Dumanoglu, A.A. (2004), "Spatial variability effects of ground motions on cable-stayed bridges", *Soil Dyn. Earthq. Eng.*, **24**, 241-250.
Soyluk, K., Dumanoglu, A.A. and Tuna, M.E. (2004), "Random vibration and deterministic analyses of cable-stayed bridges to asynchronous ground motion", *Struct. Eng. Mech.*, **18**, 231-246.
Tsai, C.S., Chen, W.S., Chiang, T.C. and Chen, B.J. (2006), "Component and shaking table tests for full-scale multiple friction pendulum system", *Earthq. Eng. Struct. Dyn.*, **35**, 1653-1675.
Wesolowsky, M.J. and Wilson, J.C. (2003), "Seismic isolation of cable-stayed bridges for near-field ground motions", *Earthq. Eng. Struct. Dyn.*, **32**, 2107-2126.
Zayas, V.A., Low, S.S., Mahin, S.A. and Bozzo, L. (1989), "Feasibility and performance studies on improving the earthquake resistance of new existing building using the friction pendulum system", In: Report No. UCB/EERC 89-09. Berkeley (CA): Earthquake Engineering and Research Center, College of Engineering, University of California.
Zembaty, Z. and Rutenberg, A. (1998), "On the sensitivity of bridge seismic response with local soil amplification", *Earthq. Eng. Struct. Dyn.*, **27**, 1095-1099.
Zerva, A. (1991), "Effect of spatial variability and propagation of seismic ground motions on the response of multiply supported structures", *Probabilist. Eng. Mech.*, **6**, 212-221.